Antiviral Research 171 (2019) 104596

Contents lists available at ScienceDirect

Antiviral Research

journal homepage: www.elsevier.com/locate/antiviral

Genetic stability of live-attenuated Zika vaccine candidates

Antonio E. Muruato[a,b,c,1], Chao Shan[d,1], Camila R. Fontes-Garfias[d], Yang Liu[d], Zengguo Cao[d], Qiang Gao[e], Scott C. Weaver[a,b,c,f,g], Pei-Yong Shi[b,c,d,f,g,*]

[a] Department of Microbiology & Immunology, University of Texas Medical Branch, Galveston, TX, USA
[b] Institute for Human Infections & Immunity, University of Texas Medical Branch, Galveston, TX, USA
[c] Institute for Translational Science, University of Texas Medical Branch, Galveston, TX, USA
[d] Department of Biochemistry & Molecular Biology, University of Texas Medical Branch, Galveston, TX, USA
[e] Sinovac Bioteck Co., Ltd., Beijing, China
[f] Sealy Institute for Vaccine Sciences, University of Texas Medical Branch, Galveston, TX, USA
[g] Sealy Center for Structural Biology & Molecular Biophysics, University of Texas Medical Branch, Galveston, TX, USA

ARTICLE INFO

Keywords:
Zika virus
Live-attenuated vaccine
Flavivirus
Virulence
Vaccine development

ABSTRACT

Zika virus (ZIKV) has drawn global attention as the etiologic agent of Zika Congenital Syndrome in babies born to infected pregnant women. To prevent future ZIKV outbreaks and protect persons at risk for severe disease, we developed two live-attenuated vaccine (LAV) candidates containing 10- or 20-nucleotide deletions in the 3′UTR of the viral genome (Δ10 and Δ20). After a single-dose immunization, both Δ10 and Δ20 LAVs protected mice and non-human primates against ZIKV infection. Here, we characterized the stability, safety, and efficacy of the LAVs after continuously culturing them on manufacture Vero cells for ten rounds. Whole genome sequencing showed that passage 10 (P10) LAVs retained the engineered Δ10 and Δ20 deletions; one to four additional mutations emerged at different regions of the genome. In A129 mice, the P10 LAVs exhibited viremia higher than the un-passaged LAVs, but lower than wild-type ZIKV; unlike wild-type ZIKV-infected mice, none of the P10 LAV-infected mice developed disease or death, demonstrating that the P10 LAVs remained attenuated. Mice immunized with a single dose of the P10 LAVs developed robust neutralizing antibody titers (1/1,000 to 1/10,000) and were protected against epidemic ZIKV challenge. The P10 LAVs did not exhibit increased neurovirulence. Intracranial inoculation of one-day-old CD1 pups with 10^3 focus-forming units of the P10 Δ10 and Δ20 LAVs resulted in 100% and ≥80% survival, respectively. Furthermore, the P10 LAVs remained incompetent in infecting *Aedes aegypti* mosquitoes after intrathoracic microinjection. Our results support the phenotypic stability and further development of these promising LAVs for ZIKV.

1. Introduction

Many viruses from *Flavivirus* genus in the family *Flaviviridae* cause significant human diseases, including Zika (ZIKV), dengue (DENV), yellow fever (TBEV), West Nile (WNV), Japanese encephalitis (JEV), and tick-borne encephalitis (TBEV) viruses. ZIKV is a positive-sense, single-stranded RNA virus originally isolated from a viremic rhesus monkey in a Uganda Forest in 1947 (Dick et al., 1952). During epidemics, it is mainly transmitted by *Aedes aegypti* and *Aedes albopictus* mosquitoes (Azar et al., 2017; Roundy et al., 2017). In infected animals and humans, ZIKV shows a tropism for a variety of tissues, such as the brain, eyes, and reproductive tract (Miner and Diamond, 2017). The shedding of infectious virus in body fluids can also lead to non-vectored transmission (Foy et al., 2011; Mead et al., 2018). ZIKV remained a neglected pathogen due to a dearth of reported outbreaks (aside from sporadic infections) until 2013, when a series of outbreaks culminated Brazil in 2015 followed by spread throughout Latin America, the Caribbean, and into the U.S. Its implication as a causative agent for microcephaly led to international concern (Driggers et al., 2016). Infection with ZIKV typically manifests in asymptomatic cases or a mild febrile illness accompanied by maculopapular rash and headache (Mittal et al., 2017). However, there is also the potential for more severe outcomes such as Guillain-Barrè Syndrome (GBS) in adults, and if following maternal infection during pregnancy, the fetus may develop

Abbreviations: ZIKV, Zika virus; 3′UTR, 3′ untranslated region; LAV, live-attenuated vaccine; Δ 10, live-attenuated vaccine containing a 3′UTR 10-nucleotide deletion; Δ 20, live-attenuated vaccine containing a 3′UTR 20-nucleotide deletion; WT, wild-type

* Corresponding author. Institute for Human Infections & Immunity, University of Texas Medical Branch, Galveston, TX, USA.
E-mail address: peshi@utmb.edu (P.-Y. Shi).

[1] A.E.M. and C.S. made equal contributions to this study.

https://doi.org/10.1016/j.antiviral.2019.104596
Received 9 August 2019; Received in revised form 30 August 2019; Accepted 2 September 2019
Available online 04 September 2019
0166-3542/

Zika Congenital Syndrome (ZCS). ZCS can manifest itself in various forms of developmental defects, including devastating outcomes of microcephaly, retinopathy, and hearing loss (Mittal et al., 2018).

Due to the potentially catastrophic course of ZIKV infection, there is urgent medical need for development of ZIKV therapeutics or vaccines, particularly for endemic areas (Shan et al., 2016a; Zou and Shi, 2019). There are currently no approved treatments or vaccines for ZIKV infection. Several vaccine strategies have been pursued, including live-attenuated virus (LAV), lipid encapsulated mRNA vaccines, DNA vectored, virus vectored, and formalin-inactivated vaccines (Abbink et al., 2016; Dowd et al., 2016; Larocca et al., 2016; Li et al., 2018a, 2018b; Pardi et al., 2017; Richner et al., 2017a, Richner et al., 2017b; Shan et al., 2017b; Xie et al., 2017). Although traditionally subunit and inactivated vaccines are considered the safest, they often require multiple doses, exhibit limited or waning efficacy over time, and require immunization boosts. In contrast, LAVs are likely to deliver single dose efficacy with long-lasting protective immunity, whereas safety hurdles can be higher (Shan et al., 2018).

Taking advantage of our ability to rationally engineer ZIKV (Shan et al., 2016b; Xie et al., 2016), we have focused on developing LAVs through modifying various genome components (Fontes-Garfias et al., 2017; Richner et al., 2017a; Shan et al., 2017a; Xie et al., 2017, 2018). One of our approaches was to attenuate ZIKV by deleting 10 or 20 nucleotides from its 3′ untranslated region (3′UTR), resulting in Δ10 and Δ20 LAVs. This 3′UTR deletion vaccine strategy has been successfully used to develop a tetravalent DENV LAV currently in phase III clinical trial (Whitehead, 2016). For ZIKV LAV development, we chose a pre-epidemic strain FSS13025 (isolated from a Cambodian patient in 2010) as the vaccine backbone because this strain is significantly less virulent than African or epidemic American strains (Xia et al., 2018b). Compared with the latter, the FSS13025 strain does not contain mutations that increase microcephaly potential (prM S17N), mosquito transmission (NS1 A188V), or innate immune suppression (NS1 A188V) (Liu et al., 2017; Xia et al., 2018a, Xia et al., 2018b; Yuan et al., 2017). Both Δ10 and Δ20 LAVs have been previously characterized for safety, efficacy, and immunogenicity in various immunocompetent and immunodeficient murine as well as non-human primate (NHP) models (Shan et al., 2017a, Shan et al., 2017b).

One safety requirement is the stability of LAV candidates during manufacture. It is important to examine the sequence stability and variation, immunogenicity, and safety of ZIKV LAVs after continuously culturing them on the manufacture cell substrate. To address this question, we serially cultured the ZIKV Δ10 and Δ20 LAVs on Vero cells for ten rounds (from P0 to P10). Whole genome sequencing was performed to monitor the engineered deletions and other potential changes at different passages (P0, P4, P7, and P10). The P10 viruses were characterized for their virulence and efficacy in mouse models. Our results showed that (i) the Δ10 and Δ20 deletions are stably retained after ten rounds of culturing on Vero cells; (ii) one-to-four additional mutations emerged after P4; (iii) the P10 LAVs did not gain neurovirulence and were fully protective against epidemic ZIKV challenge in mice; (iv) the P10 LAVs remained incompetent in infecting *Aedes aegypti* mosquitoes.

2. Materials and methods

2.1. Cells, viruses, and antibodies

Vero cells were purchased from the American Type Culture Collection (ATCC; Bethesda, MD) and cultured at 37 °C with 5% CO_2 in a high-glucose Dulbecco modified Eagle's medium (DMEM; Invitrogen, Carlsbad, CA with 10% FBS (FBS; HyClone Laboratories, Logan, UT) and 1% penicillin/streptomycin (Invitrogen, Carlsbad, CA). C6/36 cells were purchased from the American Type Culture Collection (ATCC; Bethesda, MD) and cultured at 30 °C in a Leibovit's Medium (Leibowitz; Invitrogen, Carlsbad, CA with 10% FBS (FBS; HyClone Laboratories, Logan, UT), 5% tryptose phosphate broth (Invitrogen, Carlsbad, CA), 1% 100X non-essential amino acids (Invitrogen, Carlsbad, CA), and 1% penicillin/streptomycin (Invitrogen, Carlsbad, CA). The following antibodies were used: a ZIKV-specific HMAF (hyperimmune ascitic fluid; obtained from the World Reference Center of Emerging Viruses and Arboviruses [WRCEVA] at the University of Texas Medical Branch) and an anti-mouse IgG antibody labeled with a horseradish peroxidase (KPL, Gaithersburg, MD). The ZIKV Cambodian strain FSS13025 (GenBank number KU955593.1) and Puerto Rican Strain PRVABC59 (GenBank number KU501215) were produced from infectious cDNA clones as previously reported (Shan et al., 2016b; Yang et al., 2017). The un-passaged Δ10 and Δ20 LAVs were derived from cDNA plasmids (Shan et al., 2017b) All cell lines tested negative for mycoplasma. All obtained antibodies were diluted to 1:2000 fold for the indicated assays.

2.2. Immunostaining focus-forming assay and plaque assay

The immunostaining focus-forming assay was used to quantify infectious wild-type (WT) ZIKV and LAVs. Viral samples were serially tenfold diluted in DMEM ranging from 10^1 to 10^6. For each dilution, 100 µl of each dilution was added to a 24-well plate containing ~90% confluent Vero cells. The infected cells were rocked every 15 min to confirm even coverage of the cells after infection. After 1 h of incubation, each well was added with 500 µl of methyl cellulose overlay containing 2% fetal bovine serum and 1% penicillin/streptomycin. Following 4 days of incubation at 37 °C, the overlay was aspirated; 1 ml of 50/50 methanol-acetone fixative was added to each well; and the plates were incubated at room temperature for 15 min. After the incubation, the fixative was removed; plates were washed 3 times with PBS for 15 min per wash, then blocked with 3% fetal bovine serum in PBS, and reacted with ZIKV-specific MIAF for 1 h. The plates were washed 3 times with PBS, incubated for 1 h with horseradish peroxidase-conjugated secondary antibody, and detected for presence of foci after the addition of aminoethylcarbazole substrate following the manufacturer's instructions. The infectious virus was quantified as focus-forming units (FFU).

2.3. Passaging of ZIKV Δ10 and Δ20 LAV candidates

The un-passaged Δ10 P0 and Δ20 P0 LAVs were previously described (Shan et al., 2017b). P0 aliquots (100 µl) were used to infect a T-25 flask seeded with 1×10^6 Vero cells. On day 5 post-infection (p.i.), 100 µl of culture fluid was transferred to a new T25 flask containing naïve Vero cells in 5 ml of culture medium. After ten rounds of passaging, aliquots were made and resulting viruses were designated as P10. Two independent passages were performed for each LAVs.

2.4. Stability of ZIKV Δ10 and Δ20 LAV candidates, RNA extraction, and RT-PCR

For both Δ10 and Δ20 LAVs, P0, P4, P7, and P10 viruses were subjected to whole genome sequencing. QIAmp Viral RNA Kit (Qiagen) was used to extract viral RNAs from each replicate of passaged culture fluids. SuperScript III one-step RT-PCR kits (Invitrogen) were used to amplify viral RNAs. The RT-PCR products were then subjected to DNA sequencing using the Sanger method.

2.5. Viral replication analysis

Vero cells in 12-well plates ~80% confluent were infected with ZIKV strains at an MOI of 0.01 in triplicate wells. Viral stocks were diluted to the appropriate concentration in DMEM containing 2% FBS and 1% penicillin/streptomycin. The diluted virus was added to infect cells at 100 µl volume per well. The viral inocula were removed after 1 h incubation at 37 °C. The cell monolayers were washed three times with PBS, and 1 ml DMEM medium containing 2% FBS and 1%

Table 1
Mutations from passaged Δ10 and Δ20 LAVs[a].

Vaccine	Passage	PrM	E	NS1	NS2A	NS5	3′ UTR[b]	
Δ10	**Δ10 P0**	–	–	–	–	–	–	Δ10
	Δ10 P4-1	–	–	–	–	–	–	Δ10
	Δ10 P7-1	–	–	M264L (A3279T)	–	–	–	Δ10
	Δ10 P10–1	S109P (T798C)	I43M (A1106G)	M264L (A3279T)			T10,670C	Δ10
	Δ10 P4-2	–	–	–	–	–	–	Δ10
	Δ10 P7-2		H219L (A1633T)					Δ10
	Δ10 P10–2		H219L (A1633T)	D174E (T3011G)		W637R (T9576C)		Δ10
Δ20	**Δ20 P0**	–	–	–	–	–	–	Δ20
	Δ20 P4-1	–			–			Δ20
	Δ20 P7-1	–			G187R (G4104A)			Δ20
	Δ20 P10–1	F130L (T861C)			G187R (G4104A)			Δ20
	Δ20 P4-2			–				Δ20
	Δ20 P7-2			K245M (A3223T)				Δ20
	Δ20 P10–2			K245M (A3223T)				Δ20

[a] P0, P4, P7, and P7 Δ10 and Δ20 LAVs were subjected to complete genome sequencing. Nucleotide changes that lead to deduced amino acid changes from Sanger sequencing are indicated. The nucleotide positions and changes are presented in parentheses below each amino acid changes according to ZIKV FSS13025 strain (GenBank accession number KU955593.1).
[b] All passaged viruses retained the engineered 3′UTR Δ10 and Δ20 deletions (Shan et al., 2017b).

penicillin/streptomycin was added to each well. C6/36 cells in T25-flasks of ~80% confluency were infected with indicated ZIKV at an MOI of 0.01 in triplicate flasks. Viral stocks were diluted to the appropriate concentration in Leibovitz media containing 5% tryptose phosphate broth, 1% non-essential amino acids, 2% FBS, and 1% penicillin/streptomycin. The diluted viruses were used to infect cells at the final volume of 1 ml per well. The inocula were removed after 1 h infection at 37 °C. The cell monolayers were washed three times with PBS, and 5 ml of Leibovit's media containing 5% tryptose phosphate broth, 1% non-essential amino acids, 2%FBS, and 1% penicillin/streptomycin was added to each well. The medium was collected daily for immunostaining focus assay on Vero cells as described above.

2.6. Vaccination and challenge of A129 mice

All animal experiments were approved by the University of Texas Medical Branch (UTMB) IACUC. *Ifnar1*$^{-/-}$ A129 mice were obtained from colonies maintained under specific pathogen-free conditions at UTMB. Three-week-old, mixed gender A129 mice were infected with 10^3 FFU of LAV or WT viruses through the sub-cutaneous route. Disease progression of mice was monitored and scored by clinical presentation of symptoms, such as scruffiness, squinting, lethargy, and weight loss. To measure viremia, animals were anesthetized and bled via the retro-orbital sinus every other day. On day 28 p.i., animals were bled and measured for neutralizing antibody titers using an mCherry reporter ZIKV infection assay. After animals were bled for neutralizing titers, they were challenged with 10^6 of PRVABC59 and bled for viremia on day 2 post-challenge. Serum was obtained by clarifying the collected blood at 3,380 g for 5 min and stored at −80 °C. Viral titers were determined by the immunostaining protocol described above.

2.7. Antibody neutralization assay

Neutralizing antibody titers of mouse sera were determined by an mCherry ZIKV infection assay. The sera were serially two-fold diluted starting at 1:100 in DMEM with 2% FBS and 1% penicillin/streptomycin. The diluted sera were incubated with mCherry ZIKV at 37 °C for 2 h. The antibody-virus complexes were added to infect Vero cells in 96-well plates. At 48 h p.i., the cells with mCherry fluorescence were quantified by a Cytation 5 Cell Imaging Multi-Mode Reader (Biotek). The percentage of fluorescence-positive cells in the mock-treatment controls was set at 100%. The fluorescence-positive cells from serum-treated wells were normalized to those of mock-treatment controls. A four-parameter sigmoidal (logistic) model in the software GraphPad Prism 7 was used to calculate the neutralization titers (NT_{50}).

2.8. Neurovirulence test

Neurovirulence was tested for passaged and un-passaged Δ10 and Δ20 LAVs in neonatal mice. Groups of one-day-old outbred CD-1 pups (N = 9–11; Charles River Laboratories) were injected intracranially with 10^3 FFU virus. Mice were monitored daily for signs of morbidity and mortality.

2.9. Aedes aegypti mosquito infection

The second generation *Aedes aegypti* mosquitoes, derived from a Galveston, Texas colony, were used to test potential transmission of passaged Δ10 and Δ20 LAVs. Mosquitoes held seven days after emergence from the pupal state were injected intrathoracically with 50 FFU and allowed to incubate for 14 days at 28 °C. The mosquitoes were then homogenized in DMEM with 2% FBS, 1% penicillin/streptomycin, and 1% Amphotericin B. The infection rate was determined by immunostaining. This assay gives qualitative results on positive or negative infections.

2.10. Statistical analysis

All numerical data are presented as the mean ± standard deviations. Student's t-test, ANOVA, and Kaplan Meyer survival test were used for statistical analysis.

3. Results

3.1. Genetic stability of ZIKV Δ10 and Δ20 LAVs

We tested the genetic stability of Δ10 and Δ20 LAVs by continuously culturing them on Vero cells for ten rounds, with 5 days of incubation per round. Two independent passage series were performed for each LAV. Whole genome sequencing was performed for P0, P4, P7, and P10 viruses. Table 1 summarizes the mutations detected in the passaged viruses. All passaged LAVs retained the engineered 3′UTR Δ10 or Δ20 deletions. For both Δ10 and Δ20 LAVs, no mutation was detected in P4; one amino acid change emerged in P7; and zero-to-three additional substitutions appeared in P10. Notably, no common mutations were recovered from the different passaging experiments (Table 1), suggesting that none was strongly selected. These results indicate that Δ10 and Δ20 LAVs were stable in maintaining the engineered 3′UTR deletions, and that additional changes emerged after continuously passaging them on Vero cells.

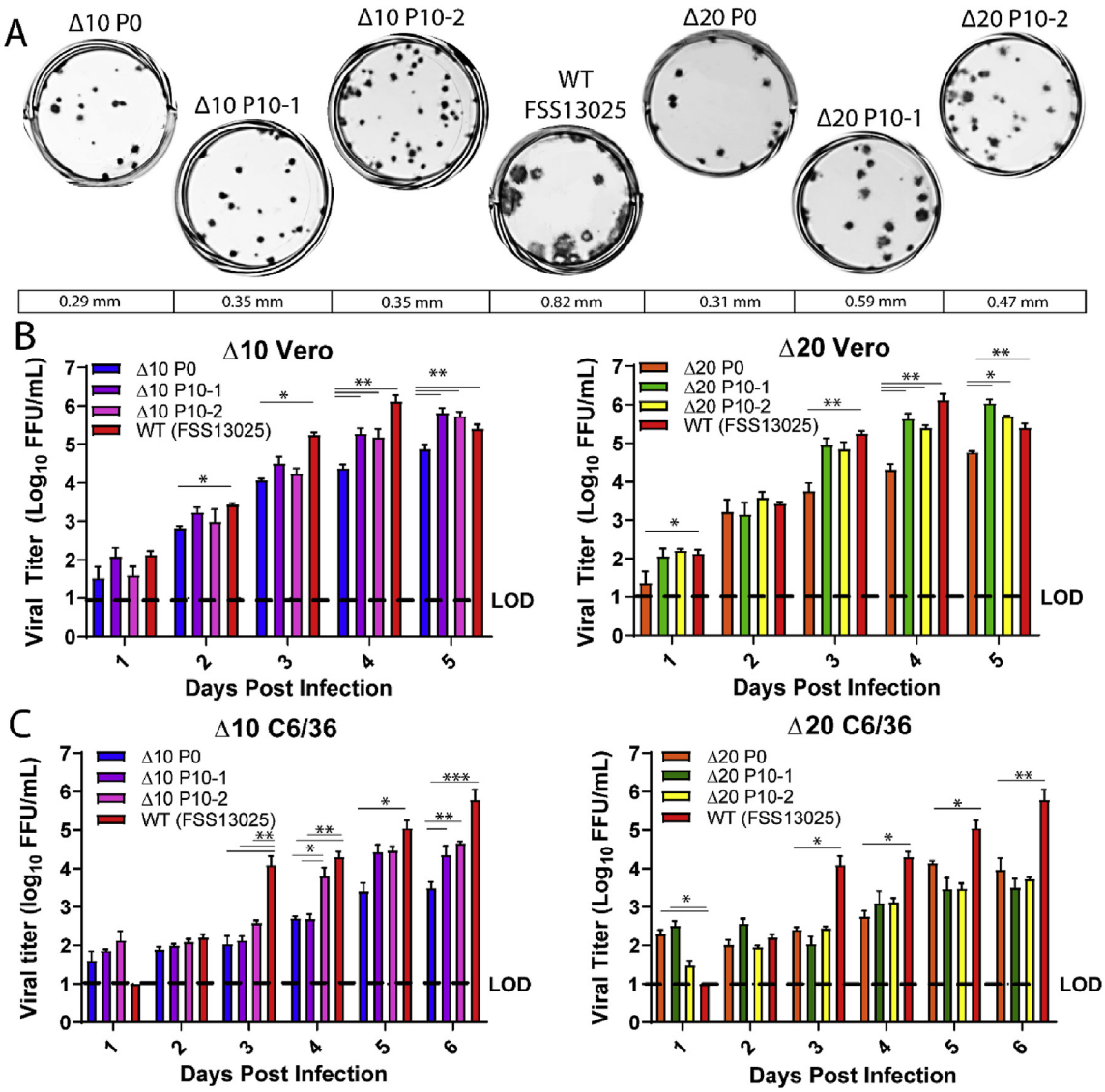

Fig. 1. Characterization of passaged Δ10 and Δ20 LAVs in cell culture. (a) Immunostaining focus-forming assay of P0 and P10 LAVs. Vero cells in 24-well plates were infected with un-passaged and passaged Δ10 or Δ20 LAVs. Immunostaining focus-forming assay were performed on day 4 post-infection. The sizes of the immunostaining foci are presented. (b) Replication kinetics of P0 and P10 LAVs and WT FSS13025 ZIKV on Vero cells. Vero cells in 24-well plates were infected with indicated viruses at an MOI of 0.01. Culture fluids were quantified using the focus-forming assay. Means and standard of deviations are presented. ANOVA followed by a Tukey's post-hoc test was performed to indicate statistical significance. * < 0.05, ** < 0.01, and *** < 0.005. (c) Replication kinetics of P0 and P10 LAVs and FSS13025 ZIKV on C6/36 cells. C6/36 cells in T25 flasks were infected with the indicated viruses at an MOI of 0.01. Culture fluids were quantified using the focus-forming assay on Vero cells. Data were derived from triplicates for each time point.

3.2. Characterization of the passaged Δ10 and Δ20 LAVs in cell culture

We characterized the replication of the P10 viruses for both Δ10 and Δ20 in cell culture. Immunostaining showed that the focus sizes of Δ10 P0 and Δ20 P0 were homogeneous on Vero cells, whereas Δ10 P10 and Δ20 P10 viruses exhibited heterogeneous focus sizes (Fig. 1A). This indicated that the mutations in Table 1 had not swept through the entire population of the P10 viruses. The focus sizes of both Δ10 P10 and Δ20 P10 were smaller than that of the WT FSS13025 ZIKV (Fig. 1A).

Next, we compared the replication kinetics of the passaged and un-passaged Δ10 and Δ20 viruses on Vero and mosquito C6/36 cells. On Vero cells, both passaged Δ10 P10 and Δ20 P10 viruses replicated to levels higher than the un-passaged P0 viruses, but lower than the WT ZIKV (Fig. 1B). On C6/36 cells, the passaged Δ10 viruses replicated to levels higher than the un-passaged viruses, but lower than the WT ZIKV (Fig. 1C, *left panel*); whereas the passaged and un-passaged Δ20 viruses replicated to similar levels (Fig. 1C, *right panel*). These results suggest the Vero-adapted mutation(s) improved viral replication in Vero cells; however, we do not know why the passaged and Δ10 P10, but not Δ20 P10, increased its replication on C6/36 cells.

3.3. The passaged and un-passaged Δ10 and Δ20 LAVs are incompetent in infecting Aedes aegypti mosquitoes

Ideally, to avoid the risk of initiating natural transmission, an arboviral LAV should not be capable of vector infection, especially when used in non-endemic location. Since Δ10 P10 showed higher replication on C6/36 cells, we examined the infectivity of the passaged and un-passaged viruses in *Aedes aegypti* mosquitoes, the major vector for ZIKV urban transmission. *Aedes aegypti* mosquitoes from Galveston, Texas were microinjected into the thorax with 50 FFU of passaged and un-passaged Δ10 or Δ20 LAVs. Intrathoracic inoculation is generally the most permissive route for arbovirus infection because it bypasses the

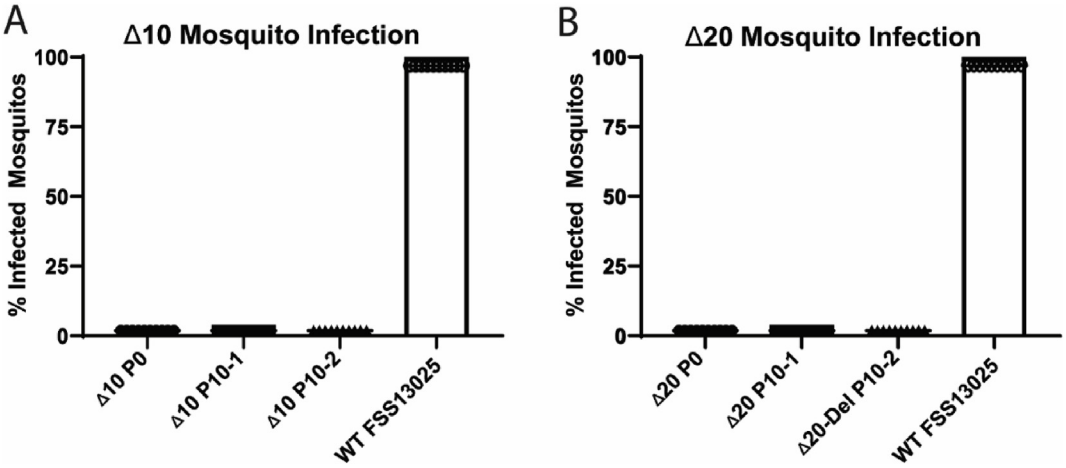

Fig. 2. Infection of *Aedes aegypti* mosquitoes via intrathoracic injection. Ten *Aedes aegypti* mosquitoes from Galveston, Texas were microinjected with 50 FFU of indicated viruses to thorax. The injected mosquitoes were reared for 14 days. Individual mosquitoes were evaluated for infectious virus by immunostaining assay which gave qualitative results on positive or negative infections.

midgut barrier (unlike oral administration). After 14 days of incubation, the microinjected mosquitoes were individually evaluated for infectious virus using an immunostaining assay. None of the passaged and un-passaged Δ10 or Δ20 viruses was detected from the microinjected mosquitoes, whereas WT FSS13025 ZIKV produced infectious virus in the injected mosquitoes (Fig. 2). The results demonstrate that neither the passaged nor the un-passaged LAVs are competent in infecting mosquitoes.

3.4. Characterization of the virulence, immunogenicity, and efficacy of passaged Δ10 and Δ20 LAVs

We next compared the safety and efficacy of the passaged and un-passaged Δ10 and Δ20 LAVs in two mouse models. First, we examined viremia, neutralizing antibody titers, and protection against epidemic ZIKV challenge in type-I interferon receptor-deficient (*Ifnar1*$^{-/-}$) A129 mice (Figs. 3A and 4A). Three-week-old mice were immunized with 1,000 FFU of passaged or un-passaged Δ10 and Δ20 LAVs. WT FSS13025 ZIKV was included as a control. Figs. 3 and 4 summarize the results of Δ10 and Δ20 LAVs in A129 mice, respectively. For both Δ10 and Δ20, the P10 viruses produced viremia kinetics intermediate between P0 LAVs and WT FSS13025 ZIKV (Figs. 3B and 4B). None of the mice that were vaccinated with passaged or un-passaged Δ10 and Δ20 LAVs exhibited any signs of disease [e.g., ruffled fur, squinty eyes, or weight loss (Figs. 3C and 4C)] or death (Figs. 3D and 4D). In contrast, the WT ZIKV-infected mice developed ruffled fur, hunched posture, weight loss (Figs. 3C and 4C) and 40% death (Figs. 3D and 4D). On day 28 post-immunization, all mice developed neutralizing antibody titers in the range of 1/1,000 to 1/10,000 (Figs. 3E and 4E). The neutralizing titers from the Δ20 groups (Fig. 4E) appeared to be higher than those from the Δ10 groups (Fig. 3E), possibly due to the slightly higher viremia in the Δ20 groups (compare Fig. 3B with Fig. 4B). As a negative control, PBS-immunized mice did not develop any neutralizing activity. After challenged with 10^6 FFU of epidemic ZIKV strain PRVABC59 on day 28 post-immunization, all mice vaccinated with passaged or un-passaged Δ10 and Δ20 LAVs were fully protected against viremia (Figs. 3F and 4F). In contrast, the PBS-immunized animals developed viremia of > 10^6 FFU/ml on day 2 post-challenge. The results indicate that Vero cell passaged Δ10 and Δ20 LAVs slightly increased viremia, but did not result in any detectable disease, and that the passaged LAVs retained immunogenicity and efficacy.

3.5. Neurovirulence of passaged Δ10 and Δ20 LAVs

Next, we tested the neurovirulence of the passaged and un-passaged Δ10 and Δ20 LAVs in neonatal mice. One-day-old outbred CD1 pups were intracranially infected with 1,000 FFU of P0 or P10 LAVs and monitored for mortality. For Δ10, 100% survival was obtained for both P0 and P10 virus-infected pups (Fig. 5, *left panel*). As positive controls, 40% and 100% mortality rates were observed for the pre-epidemic FSS13025 and epidemic PRVABC59 ZIKV-infected animals. For Δ20, pups exhibited 90%, 80%, and 90% survival rates after intracranial infection with P0, P10-1, or P10-2 virus, respectively (Fig. 5, *right panel*); statistical analysis reveals no significant difference among the three groups. These results indicate no increase of neurovirulence of Δ10 and Δ20 LAVs after ten rounds of passaging on Vero cells.

4. Discussion

The goal of this study was to examine the stability, safety, and immunogenicity of Δ10 and Δ20 LAVs on Vero cells, an approved vaccine manufacture substrate. It is critical to perform such studies to further develop these LAVs. Anez and colleagues reported that, when the DENV-4 3′UTR deletion LAV was passaged on FRhL cells (another approved cell substrate for vaccine manufacture), the passaged virus failed to elicit either viremia or neutralizing antibodies in rhesus macaques (Anez et al., 2009). An E327G mutation in the E protein that accompanied these passages increased the affinity of DENV for heparin sulfate binding, leading to reduced viral infectivity and immunogenicity. In the current study, after ten rounds of passaging on Vero cells, the engineered 3′UTR Δ10 and Δ20 deletions were stably retained. However, one-to-four additional mutations in the prM, E, NS1, NS2A, NS5 genes, or the 3′UTR, were identified in the passaged viruses (Table 1). Notably, no consensus mutations were recovered from both two independent selections in the current study, suggesting that none was strongly selected. We previously passaged the same LAVs for five rounds on Vero cells and found one-to-five amino acid mutations in the P5 viruses (which also retained the engineered 3′UTR deletions) (Shan et al., 2017b). Comparison of the two studies showed only one mutation in the E gene (H219L) that was recovered from more than one independent passages, suggesting that the observed changes may be stochastic or weakly selected under these passaging conditions.

For both Δ10 and Δ20 LAVs, the P10 viruses remained incompetent in infecting mosquitoes (Fig. 2) and did not increase their neurovirulence in one-day-old CD1 pups (Fig. 5). One remarkably safety feature of our Δ10 and Δ20 ZIKV LAVs is their low neurovirulence when

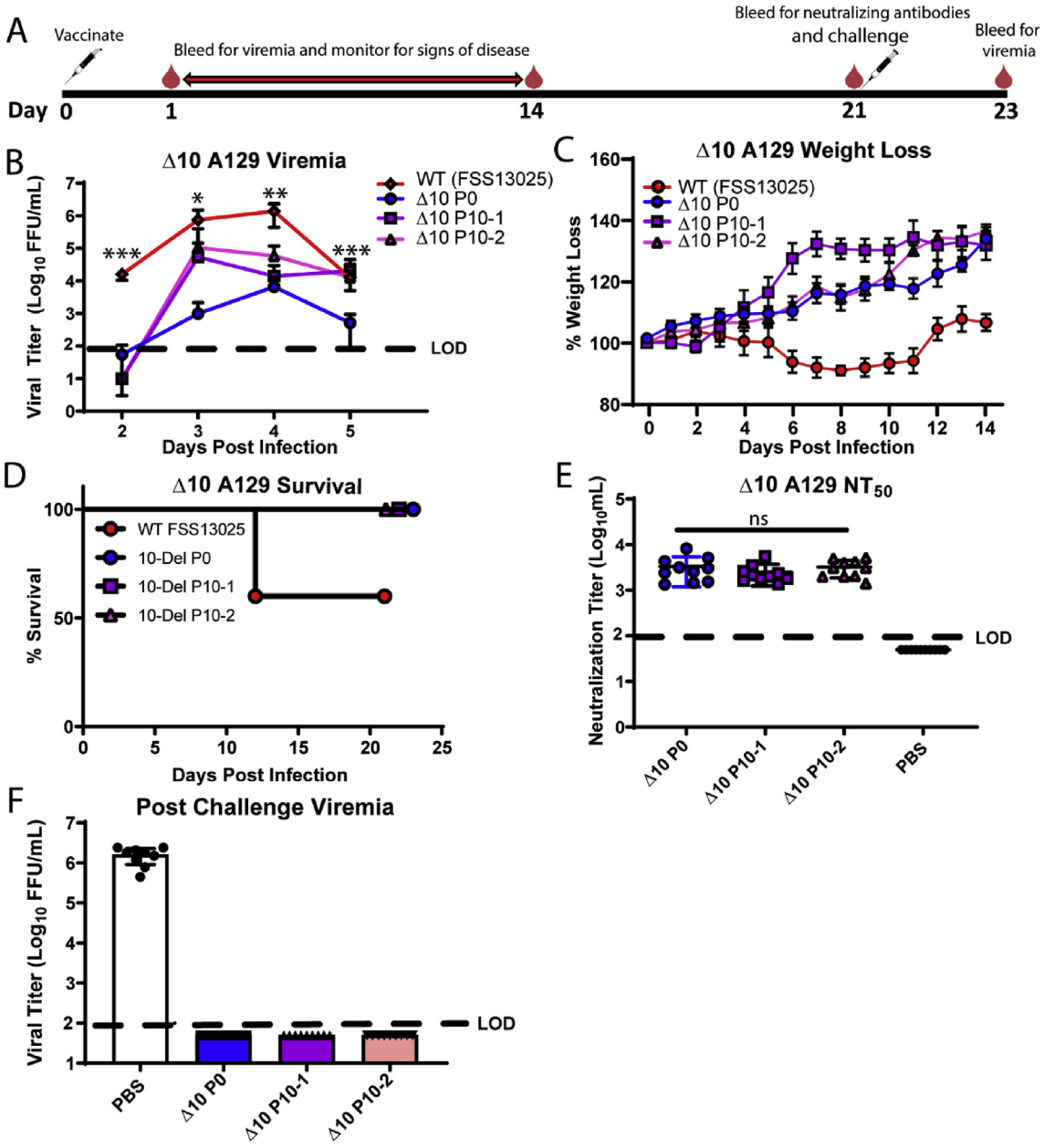

Fig. 3. Characterization of passaged Δ10 in A129 mice. (a) Experimental design. Three-week-old A129 mice (9 or 10 per group) were infected with 10^3 FFU of P10 or P0 LAVs via the subcutaneous route. WT FSS13026 ZIKV was included as a control. Viremia was measured on Vero cells using an immunostaining focus-forming assay (b). The infected mice were monitored for weight loss (c) and death (d). On day 28 p.i., the mice were bled and measured for neutralizing antibody titers using an mCherry reporter ZIKV (e). The mice were also subcutaneously challenged with 10^6 FFU of epidemic ZIKV strain (PRVABC59) on day 28 post-immunization. On day 2 post-challenging, the mice were bled and measured for viremia (f). Dotted lines indicate limit of detection (LOD). Samples with results below LOD are presented arbitrarily beneath the dotted lines. ANOVA followed by a Tukey's post-hoc test was performed to indicate statistical significance. * < 0.05, ** < 0.01, and *** < 0.005.

compared with two licensed flavivirus LAVs (YFV 17D and JEV SA14-14-2 vaccines) that cause 100% deaths in one-day-old mice (Barrett and Gould, 1986; Yun et al., 2016). A similar safety feature of low neurovirulence was observed for the DENV 3′UTR-deletion LAV candidate (Lee et al., 2011), suggesting that 3′UTR deletions may represent a reliable approach to attenuate flavivirus neurovirulence. However, more experiments in other flaviviruses are needed to test this hypothesis.

In A129 mice, all P10 viruses developed viremia higher than the P0 viruses, but lower than the WT FSS13025 virus. Mice immunized with the P10 viruses developed neutralizing antibody titers between 1/1,000 and 1/10,000 and were fully protected against WT ZIKV challenge (Figs. 3 and 4), demonstrating that the passaged Δ10 and Δ20 LAVs retained their immunogenicity and efficacy. Even though the P10 LAVs did not increase neurovirulence in neonatal mice, they generated viremia higher than the P0 LAVs, but lower than the WT FSS13025 ZIKV in A129 mice. The viremia results suggest that the mutations recovered from the P10 viruses may facilitate viral replication in the A129 mice. However, no disease, weight loss, or death was observed in the P10 LAV-infected A129 mice, whereas the WT ZIKV-infected mice developed significant weight loss and 40% death (Figs. 3 and 4), demonstrating that the passaged LAVs remained attenuated. During future development, the safety implication of the increased viremia of the P10 viruses in A129 mice should be closely monitored, including in non-

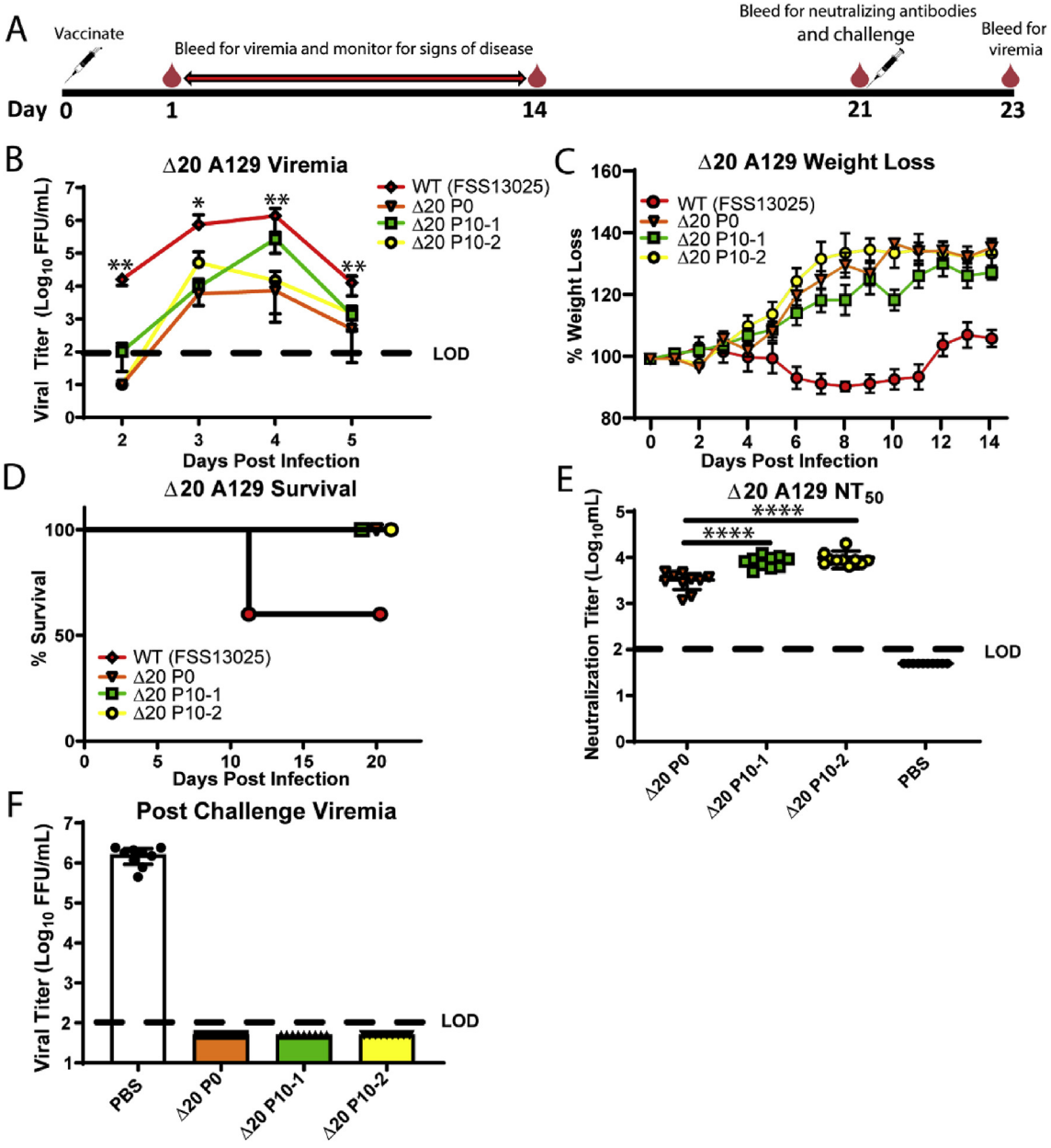

Fig. 4. Characterization of passaged Δ20 LAVs in A129 mice. All experiments were performed as described in Fig. 3. Each group had 9 to 10 mice. (a) Experimental design. (b) Viremia after three-week-old A129 were subcutaneously infected with 10^3 FFU of P10 or P0 LAVs. WT FSS13026 ZIKV was included as a control. (c) Weight loss of the infected mice. (d) Survival curves of the infected animals. (e) Neutralizing antibody titers on day 28 post-infection. (f) Protection after the immunized mice were subcutaneously challenged with 10^6 FFU of epidemic ZIKV strain (PRVABC59) on day 28 post-immunization. The viremia was measured on day 2 post-challenging. Dotted lines indicate limit of detection (LOD). Samples with results below LOD are presented arbitrarily beneath the dotted lines. ANOVA followed a Tukey's post-hoc test was performed to indicate statistical significance. * < 0.05, ** < 0.01, and *** < 0.005.

human primates. Similar studies have been reported for the DENV 3′UTR deletion LAV that is currently in phase III clinical trials (Lee et al., 2011). After culturing DENV-2/4 Δ30 (chimeric virus containing DENV-2 prM-E genes in the backbone of DENV-4 Δ30 LAV) on Vero cells for ten rounds, the P10 viruses accumulated up to ten mutations in E, NS2B, and NS3 genes; the passaged viruses increased neurovirulence in one-day-old pups and hemorrhages in four-to five-week-old mice. Collectively, the available information suggests that NHP neurovirulence testing and complete genome sequencing of the GMP batch of ZIKV Δ10 and Δ20 LAVs will be needed to ensure the safety of vaccines before their clinical development.

We recently showed that ZIKV Δ20 LAV could be efficiently launched using a DNA plasmid (Zou et al., 2018). A single-dose immunization of Δ20 plasmid as low as 0.5 μg conferred 100% sterilizing immunity in A129 mice, leading to full protection against WT ZIKV infection in both pregnant and non-pregnant mice. DNA-launched LAVs have also been reported for JEV SA14-14-2, Kunjin virus, YFV 17D, Venezuelan equine encephalitis virus TC-83 strain, and chikungunya virus 181/clone25 strain (Hall et al., 2003; Nickols et al., 2017; Tretyakova et al., 2013, 2014a, 2014b). Compared with traditional LAV production in cells or eggs, the DNA-launched technology has the advantages of chemical stability, ease of production, and no “cold chain” requirement. In addition, the DNA-lunched platform minimizes the stability concern because it eliminates the requirement of LAV manufacture in cells or eggs. The DNA-launched chikungunya vaccine also appears to generate fewer reversions of the attenuating point mutations compared to traditional virus administration (Hidajat et al., 2016). To further develop the DNA-launched ZIKV LAV platform, it is critical to

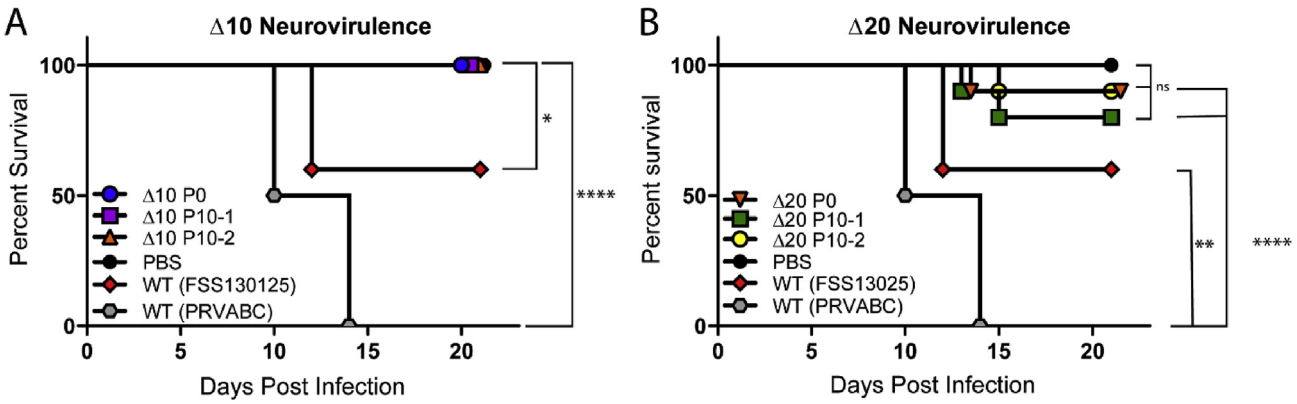

Fig. 5. Neurovirulence of passaged Δ10 and Δ20 LAVs in neonate mice. One-day-old CD1 pups (9–11 per group) were intracranially infected with 1,000 FFU of indicated virus and monitored daily for mortality for three weeks. A Kaplan Meyer survival test was performed to indicate statistical significance. * < 0.0332, ** < 0.0021, *** < 0.0002, and **** < 0.0001.

translate these promising results from mice to NHPs.

Another advantage of the DNA-launched LAV platform is the elimination of cell culture manufacture and passages for production. For a traditionally cell culture-manufactured LAV (generated from a cDNA clone), some of the Vero-adaptive mutations (Table 1) would probably need to be engineered into the cDNA clone to increase genetic stability. However, for the DNA-launched version, the lack of any cell culture passages for seed stock generation or manufacture (the plasmid is only replicated in bacteria in a high-fidelity manner) eliminates this concern.

Different vaccine platforms have distinct advantages and disadvantages (Shan et al., 2018). Given the geographic distribution of the *Aedes aegypti* vector, mostly in developing countries, a single-dose vaccine with long-lasting protective immunity is ideal to impart a profound public health impact. It is not known if the correlate of protection for maternal-to-fetal transmission during pregnancy is different from that for protection of ZIKV infection under non-pregnancy condition. Both neutralizing antibodies and T cell immunity may be important for pregnancy protection. The LAV platform could potentially fulfill these requirements through immunizing children before they reach child-bearing age. Thus, LAVs should be developed in parallel to inactivated and subunit vaccines. These complementary vaccines will provide options for different medical needs and patient risks.

5. Conclusion

The study demonstrated the stability of the 3′UTR deletions of ZIKV Δ10 and Δ20 LAVs. Although mutation(s) emerged after continuous passaging on Vero cells, they do not increase neurovirulence or change the immunogenicity and efficacy of the vaccine candidates. These results suggest that further development of these ZIKV LAV candidates is warranted.

Acknowledgements

We thank colleagues from the University of Texas of Medical Branch at Galveston for helpful discussions and support during the course of the work. P.-Y.S. was supported by NIH grants AI142759, AI127744, and AI136126; and awards from the Kleberg Foundation, John S. Dunn Foundation, Amon G. Carter Foundation, Gilson Longenbaugh Foundation, and Summerfield Robert Foundation. This research was also supported by NIH grant AI120942 and the Western Gulf Center of Excellence for Vector-Borne Diseases (CDC grant U01CK000512) to S.C.W.

References

Abbink, P., Larocca, R.A., De La Barrera, R.A., Bricault, C.A., Moseley, E.T., Boyd, M., Kirilova, M., Li, Z., Ng'ang'a, D., Nanayakkara, O., Nityanandam, R., Mercado, N.B., Borducchi, E.N., Agarwal, A., Brinkman, A.L., Cabral, C., Chandrashekar, A., Giglio, P.B., Jetton, D., Jimenez, J., Lee, B.C., Mojta, S., Molloy, K., Shetty, M., Neubauer, G.H., Stephenson, K.E., Peron, J.P., Zanotto, P.M., Misamore, J., Finneyfrock, B., Lewis, M.G., Alter, G., Modjarrad, K., Jarman, R.G., Eckels, K.H., Michael, N.L., Thomas, S.J., Barouch, D.H., 2016. Protective efficacy of multiple vaccine platforms against Zika virus challenge in rhesus monkeys. Science 353, 1129–1132.

Anez, G., Men, R., Eckels, K.H., Lai, C.J., 2009. Passage of dengue virus type 4 vaccine candidates in fetal rhesus lung cells selects heparin-sensitive variants that result in loss of infectivity and immunogenicity in rhesus macaques. J. Virol. 83, 10384–10394.

Azar, S.R., Roundy, C.M., Rossi, S.L., Huang, J.H., Leal, G., Yun, R., Fernandez-Salas, I., Vitek, C.J., Paploski, I.A.D., Stark, P.M., Vela, J., Debboun, M., Reyna, M., Kitron, U., Ribeiro, G.S., Hanley, K.A., Vasilakis, N., Weaver, S.C., 2017. Differential vector competency of Aedes albopictus populations from the americas for zika virus. Am. J. Trop. Med. Hyg. 97, 330–339.

Barrett, A.D., Gould, E.A., 1986. Comparison of neurovirulence of different strains of yellow fever virus in mice. J. Gen. Virol. 67 (Pt 4), 631–637.

Dick, G.W., Kitchen, S.F., Haddow, A.J., 1952. Zika virus. I. Isolations and serological specificity. Trans. R. Soc. Trop. Med. Hyg. 46, 509–520.

Dowd, K.A., Ko, S.Y., Morabito, K.M., Yang, E.S., Pelc, R.S., DeMaso, C.R., Castilho, L.R., Abbink, P., Boyd, M., Nityanandam, R., Gordon, D.N., Gallagher, J.R., Chen, X., Todd, J.P., Tsybovsky, Y., Harris, A., Huang, Y.S., Higgs, S., Vanlandingham, D.L., Andersen, H., Lewis, M.G., De La Barrera, R., Eckels, K.H., Jarman, R.G., Nason, M.C., Barouch, D.H., Roederer, M., Kong, W.P., Mascola, J.R., Pierson, T.C., Graham, B.S., 2016. Rapid development of a DNA vaccine for Zika virus. Science 354, 237–240.

Driggers, R.W., Ho, C.Y., Korhonen, E.M., Kuivanen, S., Jaaskelainen, A.J., Smura, T., Rosenberg, A., Hill, D.A., DeBiasi, R.L., Vezina, G., Timofeev, J., Rodriguez, F.J., Levanov, L., Razak, J., Iyengar, P., Hennenfent, A., Kennedy, R., Lanciotti, R., du Plessis, A., Vapalahti, O., 2016. Zika virus infection with prolonged maternal viremia and fetal brain abnormalities. N. Engl. J. Med. 374, 2142–2151.

Fontes-Garfias, C.R., Shan, C., Luo, H., Muruato, A.E., Medeiros, D.B.A., Mays, E., Xie, X., Zou, J., Roundy, C.M., Wakamiya, M., Rossi, S.L., Wang, T., Weaver, S.C., Shi, P.Y., 2017. Functional analysis of glycosylation of zika virus envelope protein. Cell Rep. 21, 1180–1190.

Foy, B.D., Kobylinski, K.C., Chilson Foy, J.L., Blitvich, B.J., Travassos da Rosa, A., Haddow, A.D., Lanciotti, R.S., Tesh, R.B., 2011. Probable non-vector-borne transmission of Zika virus, Colorado, USA. Emerg. Infect. Dis. 17, 880–882.

Hall, R.A., Nisbet, D.J., Pham, K.B., Pyke, A.T., Smith, G.A., Khromykh, A.A., 2003. DNA vaccine coding for the full-length infectious Kunjin virus RNA protects mice against the New York strain of West Nile virus. Proc. Natl. Acad. Sci. U.S.A. 100, 10460–10464.

Hidajat, R., Nickols, B., Forrester, N., Tretyakova, I., Weaver, S., Pushko, P., 2016. Next generation sequencing of DNA-launched Chikungunya vaccine virus. Virology 490, 83–90.

Larocca, R.A., Abbink, P., Peron, J.P., Zanotto, P.M., Iampietro, M.J., Badamchi-Zadeh, A., Boyd, M., Ng'ang'a, D., Kirilova, M., Nityanandam, R., Mercado, N.B., Li, Z., Moseley, E.T., Bricault, C.A., Borducchi, E.N., Giglio, P.B., Jetton, D., Neubauer, G., Nkolola, J.P., Maxfield, L.F., De La Barrera, R.A., Jarman, R.G., Eckels, K.H., Michael, N.L., Thomas, S.J., Barouch, D.H., 2016. Vaccine protection against Zika virus from Brazil. Nature 536, 474–478.

Lee, H.C., Yen, Y.T., Chen, W.Y., Wu-Hsieh, B.A., Wu, S.C., 2011. Dengue type 4 live-attenuated vaccine viruses passaged in vero cells affect genetic stability and dengue-induced hemorrhaging in mice. PLoS One 6, e25800.

Li, A., Yu, J., Lu, M., Ma, Y., Attia, Z., Shan, C., Xue, M., Liang, X., Craig, K., Makadiya, N., He, J.J., Jennings, R., Shi, P.Y., Peeples, M.E., Liu, S.L., Boyaka, P.N., Li, J., 2018a. A Zika virus vaccine expressing premembrane-envelope-NS1 polyprotein. Nat. Commun. 9, 3067.

Li, X.F., Dong, H.L., Wang, H.J., Huang, X.Y., Qiu, Y.F., Ji, X., Ye, Q., Li, C., Liu, Y., Deng, Y.Q., Jiang, T., Cheng, G., Zhang, F.C., Davidson, A.D., Song, Y.J., Shi, P.Y., Qin, C.F., 2018b. Development of a chimeric Zika vaccine using a licensed live-attenuated

flavivirus vaccine as backbone. Nat. Commun. 9, 673.
Liu, Y., Liu, J., Du, S., Shan, C., Nie, K., Zhang, R., Li, X.F., Zhang, R., Wang, T., Qin, C.F., Wang, P., Shi, P.Y., Cheng, G., 2017. Evolutionary enhancement of Zika virus infectivity in Aedes aegypti mosquitoes. Nature 545, 482–486.
Mead, P.S., Duggal, N.K., Hook, S.A., Delorey, M., Fischer, M., Olzenak McGuire, D., Becksted, H., Max, R.J., Anishchenko, M., Schwartz, A.M., Tzeng, W.P., Nelson, C.A., McDonald, E.M., Brooks, J.T., Brault, A.C., Hinckley, A.F., 2018. Zika virus shedding in semen of symptomatic infected men. N. Engl. J. Med. 378, 1377–1385.
Miner, J.J., Diamond, M.S., 2017. Zika virus pathogenesis and tissue tropism. Cell Host Microbe 21, 134–142.
Mittal, R., Fifer, R.C., Liu, X., 2018. A possible association between hearing loss and zika virus infections. JAMA Otolaryngology–Head & Neck Surgery 144, 3–4.
Mittal, R., Fifer, R.C., Liu, X.Z., 2017. A possible association between hearing loss and zika virus infections. JAMA Otolaryngol Head Neck Surg 2168-6181.
Nickols, B., Tretyakova, I., Tibbens, A., Klyushnenkova, E., Pushko, P., 2017. Plasmid DNA launches live-attenuated Japanese encephalitis virus and elicits virus-neutralizing antibodies in BALB/c mice. Virology 512, 66–73.
Pardi, N., Hogan, M.J., Pelc, R.S., Muramatsu, H., Andersen, H., DeMaso, C.R., Dowd, K.A., Sutherland, L.L., Scearce, R.M., Parks, R., Wagner, W., Granados, A., Greenhouse, J., Walker, M., Willis, E., Yu, J.S., McGee, C.E., Sempowski, G.D., Mui, B.L., Tam, Y.K., Huang, Y.J., Vanlandingham, D., Holmes, V.M., Balachandran, H., Sahu, S., Lifton, M., Higgs, S., Hensley, S.E., Madden, T.D., Hope, M.J., Kariko, K., Santra, S., Graham, B.S., Lewis, M.G., Pierson, T.C., Haynes, B.F., Weissman, D., 2017. Zika virus protection by a single low-dose nucleoside-modified mRNA vaccination. Nature 543 (7644), 248–251.
Richner, J.M., Himansu, S., Dowd, K.A., Butler, S.L., Salazar, V., Fox, J.M., Julander, J.G., Tang, W.W., Shresta, S., Pierson, T.C., Ciaramella, G., Diamond, M.S., 2017. Modified mRNA vaccines protect against zika virus infection. Cell (2), 273–283.
Richner, J., Jagger, B., Shan, C., Fontes, C., Dowd, K., Cao, B., Himansu, S., Caine, E., Nunes, B., Medeiros, D., Muruato, A., Foreman, B., Luo, H., Wang, T., Barrett, A., Weaver, S., Vasconcelos, P., Rossi, S., Ciaramella, G., Mysorekar, I., Pierson, T., Shi, P., Diamond, M., 2017a. Vaccine mediated protection against Zika virus induced congenital disease. Cell 170, 273–283.
Roundy, C.M., Azar, S.R., Rossi, S.L., Huang, J.H., Leal, G., Yun, R., Fernandez-Salas, I., Vitek, C.J., Paploski, I.A., Kitron, U., Ribeiro, G.S., Hanley, K.A., Weaver, S.C., Vasilakis, N., 2017. Variation in Aedes aegypti mosquito competence for zika virus transmission. Emerg. Infect. Dis. 23, 625–632.
Shan, C., Muruato, A.E., Jagger, B.W., Richner, J., Nunes, B.T.D., Medeiros, D.B.A., Xie, X., Nunes, J.G.C., Morabito, K.M., Kong, W.P., Pierson, T.C., Barrett, A.D., Weaver, S.C., Rossi, S.L., Vasconcelos, P.F.C., Graham, B.S., Diamond, M.S., Shi, P.Y., 2017a. A single-dose live-attenuated vaccine prevents Zika virus pregnancy transmission and testis damage. Nat. Commun. 8, 676.
Shan, C., Muruato, A.E., Nunes, B.T., Luo, H., Xie, X., Medeiros, D.B., Wakamiya, M., Tesh, R.B., Barrett, A.D., Wang, T., Weaver, S.C., Vasconcelos, P.F., Rossi, S.L., Shi, P.Y., 2017b. A live-attenuated Zika virus vaccine candidate induces sterilizing immunity in mouse models. Nat. Med. 36, 92–102.
Shan, C., Xie, X., Barrett, A.D.T., Garcia-Blanco, M.A., Tesh, R.B., Vasconcelos, P.F.C., Vasilakis, N., Weaver, S.C., Shi, P.Y., 2016a. Zika virus: diagnosis, therapeutics, and vaccine. ACS Infect. Dis. 2, 170–172.
Shan, C., Xie, X., Muruato, A.E., Rossi, S.L., Roundy, C.M., Azar, S.R., Yang, Y., Tesh, R.B., Bourne, N., Barrett, A.D., Vasilakis, N., Weaver, S.C., Shi, P.Y., 2016b. An infectious cDNA clone of zika virus to study viral virulence, mosquito transmission, and antiviral inhibitors. Cell Host Microbe 19, 891–900.
Shan, C., Xie, X., Shi, P.Y., 2018. Zika virus vaccine: progress and challenges. Cell Host Microbe 24, 12–17.
Tretyakova, I., Hearn, J., Wang, E., Weaver, S., Pushko, P., 2014a. DNA vaccine initiates replication of live attenuated chikungunya virus in vitro and elicits protective immune response in mice. J. Infect. Dis. 209, 1882–1890.
Tretyakova, I., Lukashevich, I.S., Glass, P., Wang, E., Weaver, S., Pushko, P., 2013. Novel vaccine against Venezuelan equine encephalitis combines advantages of DNA immunization and a live attenuated vaccine. Vaccine 31, 1019–1025.
Tretyakova, I., Nickols, B., Hidajat, R., Jokinen, J., Lukashevich, I.S., Pushko, P., 2014b. Plasmid DNA initiates replication of yellow fever vaccine in vitro and elicits virus-specific immune response in mice. Virology 468–470, 28–35.
Whitehead, S.S., 2016. Development of TV003/TV005, a single dose, highly immunogenic live attenuated dengue vaccine; what makes this vaccine different from the Sanofi-Pasteur CYD vaccine? Expert Rev. Vaccines 15, 509–517.
Xia, H., Luo, H., Shan, C., Muruato, A.E., Nunes, B.T.D., Medeiros, D.B.A., Zou, J., Xie, X., Giraldo, M.I., Vasconcelos, P.F.C., Weaver, S.C., Wang, T., Rajsbaum, R., Shi, P.Y., 2018a. An evolutionary NS1 mutation enhances Zika virus evasion of host interferon induction. Nat. Commun. 9, 414.
Xia, H., Xie, X., Shan, C., Shi, P.Y., 2018. Potential mechanisms for enhanced zika epidemic and disease. ACS Infect. Dis. 4 (5), 656–659.
Xie, X., Kum, D.B., Xia, H., Luo, H., Shan, C., Zou, J., Muruato, A.E., Medeiros, D.B.A., Nunes, B.T.D., Dallmeier, K., Rossi, S.L., Weaver, S.C., Neyts, J., Wang, T., Vasconcelos, P.F.C., Shi, P.Y., 2018. A single-dose live-attenuated zika virus vaccine with controlled infection rounds that protects against vertical transmission. Cell Host Microbe 24, 487–499 e485.
Xie, X., Yang, Y., Muruato, A.E., Zou, J., Shan, C., Nunes, B.T., Medeiros, D.B., Vasconcelos, P.F., Weaver, S.C., Rossi, S.L., Shi, P.Y., 2017. Understanding zika virus stability and developing a chimeric vaccine through functional analysis. mBio 8.
Xie, X., Zou, J., Shan, C., Yang, Y., Kum, D.B., Dallmeier, K., Neyts, J., Shi, P.Y., 2016. Zika virus replicons for drug discovery. EBioMedicine 12, 156–160.
Yang, Y., Shan, C., Zou, J., Muruato, A.E., Bruno, D.N., de Almeida Medeiros Daniele, B., Vasconcelos, P.F., Rossi, S.L., Weaver, S.C., Xie, X., Shi, P.Y., 2017. A cDNA clone-launched platform for high-yield production of inactivated zika vaccine. EBioMedicine 17, 145–156.
Yuan, L., Huang, X.Y., Liu, Z.Y., Zhang, F., Zhu, X.L., Yu, J.Y., Ji, X., Xu, Y.P., Li, G., Li, C., Wang, H.J., Deng, Y.Q., Wu, M., Cheng, M.L., Ye, Q., Xie, D.Y., Li, X.F., Wang, X., Shi, W., Hu, B., Shi, P.Y., Xu, Z., Qin, C.F., 2017. A single mutation in the prM protein of Zika virus contributes to fetal microcephaly. Science 358, 933–936.
Yun, S.I., Song, B.H., Polejaeva, I.A., Davies, C.J., White, K.L., Lee, Y.M., 2016. Comparison of the live-attenuated Japanese encephalitis vaccine SA14-14-2 strain with its pre-attenuated virulent parent SA14 strain: similarities and differences in vitro and in vivo. J. Gen. Virol. 97, 2575–2591.
Zou, J., Shi, P.Y., 2019. Strategies for Zika drug discovery. Curr Opin Virol 35, 19–26.
Zou, J., Xie, X., Luo, H., Shan, C., Muruato, A.E., Weaver, S.C., Wang, T., Shi, P.Y., 2018. A single-dose plasmid-launched live-attenuated Zika vaccine induces protective immunity. EBioMedicine 36, 92–102.